Heliyon 9 (2023) e16072

Contents lists available at ScienceDirect

Heliyon

journal homepage: www.cell.com/heliyon

Research article

Size controlled biosynthesis of silver nanoparticles using *Ophiorrhiza mungos, Ophiorrhiza harrisiana* and *Ophiorrhiza rugosa* aqueous leaf extract and their antimicrobial activity

Sumon Ganguli [a,b], Sabbir Howlader [a,b], A.K.M. Atique Ullah [c], Farhana Rumzum Bhuiyan [d], Aklima A. Akhi [a,b], Abid Hasan [a,b], Kamol Dey [a], Saiful Islam [e], Ferdousi Ali [f], Ashok Kumar Chakraborty [g], Samiran Bhattacharjee [h,*], Benu Kumar Dey [i,**]

[a] *Department of Applied Chemistry and Chemical Engineering, University of Chittagong, Chattogram, 4331, Bangladesh*
[b] *Biomaterials Research Laboratory (BRL), Department of Applied Chemistry and Chemical Engineering, University of Chittagong, Chattogram, 4331, Bangladesh*
[c] *Nanoscience and Technology Laboratory, Atomic Energy Center, Bangladesh Atomic Energy Commission, Dhaka, 1000, Bangladesh*
[d] *Laboratory of Biotechnology and Molecular Biology, Department of Botany, University of Chittagong, Chattogram, 4331, Bangladesh*
[e] *Industrial Microbiology Research Division, Bangladesh Council of Scientific and Industrial Resaerch (BCSIR), Chattogram Laboratories, Chattogram, 4220, Bangladesh*
[f] *Department of Microbiology, University of Chittagong, Chattogram, 4331, Bangladesh*
[g] *Department of Applied Chemistry and Chemical Engineering, Islamic University, Kushtia, 7003, Bangladesh*
[h] *Centre for Advanced Research in Sciences (CARS), University of Dhaka, Dhaka, 1000, Bangladesh*
[i] *Department of Chemistry and Pro-Vice-Chancellor (Academic), University of Chittagong, Chattogram, 4331, Bangladesh*

ARTICLE INFO

Keywords:
Green synthesis
Silver nanoparticles
Ophiorrhiza genus
Plant extract
Antibacterial activity
Antifungal activity

ABSTRACT

In this work, the aqueous leaf extracts of three *Ophiorrhiza* genus species, namely *Ophiorrhiza mungos* (*Om*), *Ophiorrhiza harrisiana* (*Oh*) and *Ophiorrhiza rugosa* (*Or*), have been used as the reducing and capping agents to control the size of AgNPs, *Om*-AgNPs, *Oh*-AgNPs and *Or*-AgNPs, respectively and found to be an effective antimicrobial agent against a wide range of bacteria and fungi. The biosynthesized AgNPs were studied by UV–Visible spectrophotometer, powder X-ray diffraction (XRD), scanning electron microscopy (SEM), energy dispersive X-ray, transmission electron microscopy (TEM) and Fourier transform infrared spectrometer (FTIR). The average particle sizes of *Om*-AgNPs, *Oh*-AgNPs and *Or*-AgNPs were measured as 17 nm, 22 nm and 26 nm, respectively, and observed to be spherical and face-centered cubic crystals. The antibacterial test of synthesized AgNPs was performed against *Staphylococcus aureus*, *Bacillus cereus*, *Escherichia coli*, and *Vibrio cholerae* where the maximum antibacterial activity was observed by reducing the nano-size and increasing the silver content of AgNPs. The antifungal effect of these three types of AgNPs on *Penicillium notatum* and *Aspergillus niger* was also evaluated and their growth with AgNPs concentrations of 450 μg/mL was inhibited up to 80–90% and 55–70%, respectively. The size-control synthesis of AgNPs using the *Ophiorrhiza* genus species is presented here for the first time where the synthesized AgNPs showed higher stability and antimicrobial activities. Therefore, this study might lead to synthesize AgNPs with different morphologies using plant extracts of

* Corresponding author. .
** Corresponding author.
E-mail addresses: s.bhattacharjee@du.ac.bd (S. Bhattacharjee), benudey@yahoo.com (B.K. Dey).

https://doi.org/10.1016/j.heliyon.2023.e16072
Received 8 February 2023; Received in revised form 28 April 2023; Accepted 4 May 2023
Available online 6 May 2023

the same genus but from different species and provide strong encouragement for future applications in treating infectious diseases.

1. Introduction

Nanotechnology is used to improve the properties of the material by manipulating its structure at the nanoscale for developing innovative materials and technologies with distinctive features [1]. These particles have unique characteristics that are entirely different from those of the bulk because they are tiny and have a high surface area-to-volume ratio [2,3]. Nanomaterials offer answers to numerous technological and environmental problems because of their various magnetic, electrical, and optical capabilities [4]. Because of their unique properties, they can be applied in case of drugs, manufacturing and/or tailoring of materials, electronics, mechanics, antimicrobials, optics, catalysis, electronics, sensing, energy harvesting and environment and so on [3,5]. Specially, noble metals like Au, Ag, Pt etc. And their oxides, sulfides are most applied because of their extrinsic applications but among them, silver nanoparticles (AgNPs) are more advantageous in the case of biomedical applications [1,6]. AgNPs act at the membrane level because they can pass through the outer membrane and accumulate in the inner membrane [7]. According to another proposed mechanism, AgNPs can affect the structure of a cell's membrane in addition to breaking through it [8,9]. Furthermore, In addition to being highly effective against both Gram-negative and Gram-positive bacterial strains, AgNPs are also used as photocatalysts, biopesticides, and biosensors [10]. AgNPs act as adsorbents to remove dye, antioxidant, anti-inflammatory, anticoagulant, anticoagulant, wound healing, anticancer etc. purposes [11–13]. Again, AgNPs can be considered one of the widely studied nanomaterials and therefore have been chosen for our study.

However, the conventional physical (e.g., mechanical milling, laser ablation, sputtering) and chemical (e.g., chemical reduction, electrochemical precipitation, vapor deposition, pyrolysis, atomic condensation) methods of synthesizing AgNPs involve the use of toxic solvents and hazardous chemicals posing a great threat on the environment [14–17]. Besides, these synthesis procedures are time-consuming and require sophisticated instrumental set up which may not be cost-effective [18]. Stabilization of the synthesized AgNPs is a great concern. Thus, researchers developed unique "green chemistry" methodologies for producing nanomaterials in biological systems like bacteria, fungi, and plant extract in response to the escalating environmental concerns [19–21]. Moreover, using microorganisms in the synthesis of AgNPs is time-consuming, consists of several preparative steps, and is subsequently expensive [22]. Accounting for all aspects of readily scalable, less expensive, and rapid procedure, green synthesis using plant extract was the most prominent method for AgNPs synthesis [23,24]. Plant extract contains a wide range of biomolecules, viz., phenolic acids, flavonoids, xanthones, and phloroglucinols, which can act as reducing, capping, and stabilizing agents [25,26]. Noteworthy that, the overall characteristics of the nanoparticles are influenced by the chemical composition, size, shape and surface charge [27]. Especially, biomedical applications of AgNPs are notably size and shape-dependent [28]. Smaller AgNPs can exhibit the largest dose- and time-dependent antibacterial activity [29,30]. The size and shape can be controlled by varying pH, synthesis temperature, and reaction time [31,32]. In plant extract-based methods, different plants have different reducing, capping, and stabilizing agents to generate an enormous range of shapes and sizes, which are significant features for several biomedical applications [33,34]. Hence, the synthesis of AgNPs with variable sizes using plant extract under an eco-friendly route is highly desirable.

Genus *Ophiorrhiza* belonged to the *Rubiaceae* family is commonly found in the wet forests of Asia, Australia, New Guinea and the Pacific Islands. This genus containing 321 species, 5 varieties and 1 subspecies, is used in both traditional and modern medicine for its medicinal properties (antioxidant, antitussive and analgesic agent) and to treat snakebite, stomatitis, ulcers, inflammation, pain, cancer, wounds and bacterial and viral infections [26,35–37]. As mentioned above, the *Ophiorrhiza* plant extract is full of various biomolecules [38]. The aim of this study is to prepare various sizes of AgNPs using plant extract under eco-friendly route. The presence of various bio-chemicals in plant species of the *Ophiorrhiza* genus encouraged us to test the usefulness of functional groups of bio-chemicals for the green synthesis of AgNPs as a potential antimicrobial agent in treating infectious diseases. In this work, we have selected the three plant species of the *Ophiorrhiza* genus viz., *Ophiorrhiza mungos* (*Om*), *Ophiorrhiza harrisiana* (*Oh*) and *Ophiorrhiza rugosa* (*Or*) (Fig. 1a–c), which having different biomolecules, may be responsible for the formation of different size of AgNPs [26,35,38]. These three plant species are commonly available in the hilly area of University of Chittagong (Chattogram, Bangladesh). We

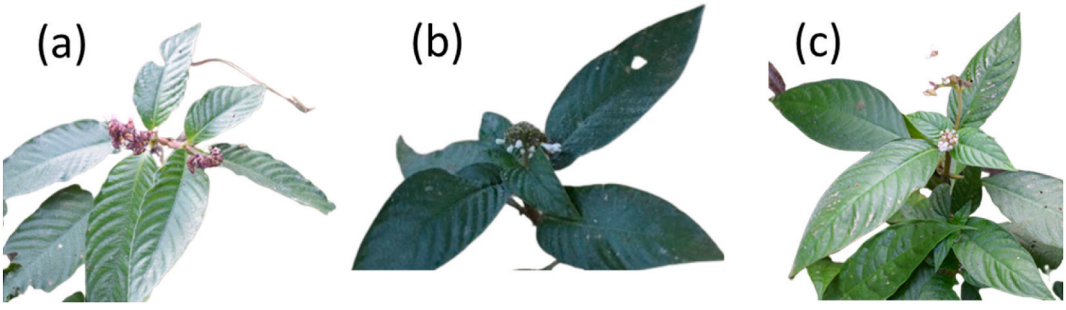

Fig. 1. Image of (a) *Ophiorrhiza mungos*, (b) *Ophiorrhiza harrisiana* and (c) *Ophiorrhiza rugosa* leaf along with its flower and stem.

describe the synthesis of highly stable AgNPs at different sizes from the aqueous leaf extracts of three *Ophiorrhiza* species, *Om-AgNPs, Oh-AgNPs* and *Or-AgNPs.* At the same time, we also highlighted its action as the effective antibacterial and antifungal agents against a wide range of bacteria and fungi namely *Staphylococcus aureus*, *Bacillus cereus*, *Escherichia coli*, *Vibrio cholera*, *Penicillium notatum* and *Aspergillus niger* which usually responsible for human diseases. To our knowledge, the formation of different sizes of AgNPs using the same plants of *Ophiorrhiza* genus and their antimicrobial activities has not been previously reported. Thus, we aimed to use the aqueous leaf extract of three *Ophiorrhiza* genus species (*Om, Oh and Or*) which have been used for the first time as the reducing and capping agents to control the size of AgNPs. In addition, their antimicrobial potential against a wide range of bacteria and fungi have been investigated.

2. Material and methods

2.1. Materials

$AgNO_3$ and Trypan blue stain solution (4%) were obtained from Merck, Germany and Bio Rad, Hercules (CA, USA), respectively, and used as received. Bactotrypton, bacto agar and yeast extract were obtained from Difco Laboratories (Detroit, MI, USA). Sodium chloride was acquired from Wako (Osaka, Japan). Fresh leaves of the plants (*Ophiorrhiza rugosa, Ophiorrhiza mungos* and *Ophiorrhiza harrisiana*) were obtained from the hilly area of the University of Chittagong (Chattogram, Bangladesh). These plants were identified and acknowledged by Farhana Rumzum Bhuiyan, Assistant Professor, Dept. of Botany, University of Chittagong, Bangladesh. Analytical-grade reagents were utilized throughout.

2.2. Leaf extracts preparation

The extraction procedure was performed following the literature with slight modifications [39]. A scheme of the biosynthesis of AgNPs is shown in Fig. 2. Each of the plant leaves was carefully washed with tap water and double distilled water, and placed for drying under sunlight, then powdered. Individually, 1.0 g of dried leaf powder with 100 mL deionized water blended under continuous stirring at 80 °C for 30 min. Whatman No. 1 filter paper was then used to separate and filter the supernatant, which was then preserved in a sealed container and maintained in a cooler until use.

2.3. Synthesis of AgNPs

AgNPs were synthesized using the methodology reported by Ullah et al. [40]. Briefly, the AgNPs were successfully synthesized using the leaf extracts of three different *Ophiorrhiza* species separately. Briefly, 20 mL of each plant extract was added in a drop-wise

Fig. 2. Schematic representation of the synthesis of AgNPs from the aqueous leaf extracts of three Ophiorrhiza species.

manner (20 min) to the 100 mL aqueous solution of $AgNO_3$ (1 mM) with continuous stirring for 60 min at 80 °C. For complete bio-reduction, the resulting liquor was preserved for 24 h at room temperature. After 24 h, the solution was centrifuged at 5000 rpm for 20 min. The paste obtained was washed three times to eliminate any contaminants and dried at 60 °C for 12 h. The product (AgNPs) was then stored in a sealed glass vial, and reserved in a desiccator until needed. The samples are denoted as *Om*-AgNPs, *Oh*-AgNPs and *Or*-AgNPs for the *Om*-, *Oh*- and *Or*-mediated plant extract, respectively.

2.4. Characterization of AgNPs

For optical characterization, UV–visible spectrophotometer (UV-1800, Shimadzu, Japan) was used. X-ray diffraction (XRD) analysis was conducted to determine the AgNPs' crystalline phase using Rigaku Ultima IV diffractometer with Cu-Kα ($\lambda = 1.5406$ Å) radiation at 0.2 min^{-1}. Fourier Transform Infrared Spectrophotometer (FTIR) spectra were measured as KBr discs on an IR Prestige (Shimadzu) spectrometer to identify the presence of the functional group. Using Scanning Electron Microscope (SEM) (JSM-6490 L A), the surface morphology of AgNPs was investigated, while the average particle size and distribution were determined by Transmission Electron Microscope (TEM) (FEI, Bellaterra Spain). To check the elemental composition, the Energy-dispersive X-ray (EDX) was employed using a BRUKER system attached to the SEM.

2.5. Antibacterial and antifungal test

The disc diffusion method was applied to identify the antibacterial activity of the synthesized AgNPs following the standard protocol [40]. *Staphylococcus aureus* (ATCC 12228), *Bacillus cereus* (ATCC 14579), *Escherichia coli* (ATCC 25922), and *Vibrio cholerae* (ATCC 39315) were assessed for the antibacterial activity of the AgNPs. On the other hand, the antifungal activity was tested employing the poisoned food technique using potato dextrose agar (PDA) as the culture medium [41]. Briefly, a sterilized pipette was used to transfer 0.5 mL of each solution into separate sterile petri dishes after *Om*-AgNPs, *Oh*-AgNPs and *Or*-AgNPs had been dispersed in deionized water. Then, the medium (20 mL) was added to each Petri dish and let to set. The middle of each petri-dish was then injected with a 5 mm mycelium block of each fungus which was positioned in an upside-down posture. Three days after incubation at 27 ± 2 °C the mycelial growth was assessed. The measurements were carried out three times and the average values were plotted.

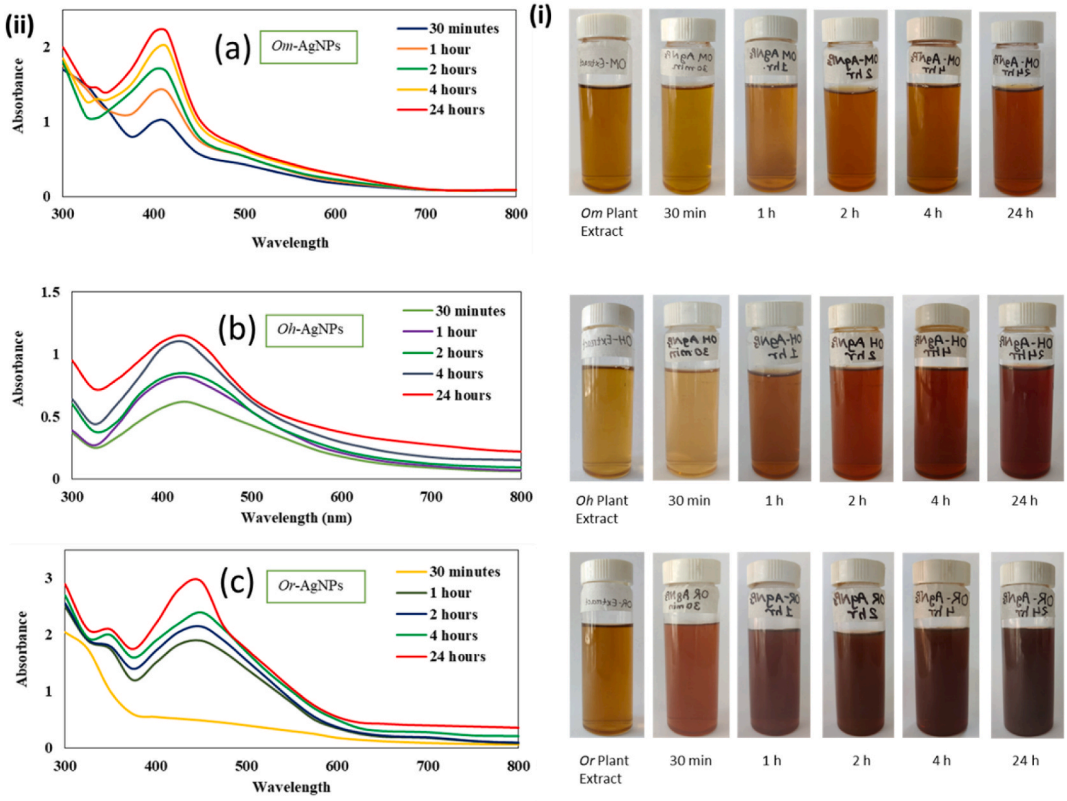

Fig. 3. (I) Color change during the formation of AgNPs. Plant extract without $AgNO_3$ solution *Om*, *Oh* and *Or*. Plant extract with $AgNO_3$ solution after 30 min, 1 h, 2 h, 4 h and 24 h. (ii) UV–Visible absorption spectra of the synthesized AgNPs (a) *Om*-AgNPs, (b) *Oh*-AgNPs and (c) *Or*-AgNPs formation at different time intervals.

3. Results and discussion

3.1. Visual examination and UV–visible spectral analysis

The green synthesis of AgNPs was performed using aqueous leaf extract of three *Ophiorrhiza* species and 1 mM of $AgNO_3$ at 80 °C. The aqueous leaf extract of *Om, Oh* and *Or* exhibited a slightly acidic nature of pH at 6.1, 5.7, and 5.8, respectively. The pH of the colloidal AgNPs solution was reached at ~4.7 after 1 h reaction between plant extract and $AgNO_3$, and then remained virtually the same afterward. To examine the formation of nanoparticles, a visual examination and UV–visible spectroscopy analysis were carried out. The visual color change of the plant extract solution from yellow to deep brown during synthesis (Fig. 3 i) owing to a surface plasmon resonance (SPR) of the bio-reduction of Ag^{+} to Ag^{0} [42].

UV–visible spectroscopy analysis is commonly applied to assess the structural characterization of nanoparticle. The reaction profile for *Om-*, *Oh-* and *Or*-mediated AgNPs as a function of time is shown in Fig. 3 ii (a - c). The SPR bands were observed at 413, 424 and 451 nm for *Om-, Oh-* and *Or*-mediated AgNPs, respectively, and the absorption intensity increased gradually with increasing reaction time up to 24 h incubation. The reaction was continued further and the Ag peak's intensity did not change. The peak position is unchanged during the reaction time, indicating that nucleation of AgNPs starts with time and the size remains unaffected during the reaction. UV–visible spectra of synthesized AgNPs were found to be coherent with Mie theory. A single SPR band was found at 413 nm, 424 nm and 451 nm for *Om*-AgNPs, *Oh*-AgNPs and *Or*-AgNPs, respectively, where average particle sizes were calculated as 18 nm, 22 nm 26 nm, respectively. Another group of researchers made identical assignments for the formation AgNPs using the surface plasmon resonance peak of AgNPs [43,44].

Literature surveys showed that the three species of plant extracts contain various phytochemicals [26,35]. The size-control synthesis of AgNPs may be due to different biomolecules, which play a vital role as reducing, capping and stabilizing agents for the growth of various sizes of AgNPs. Previous work demonstrated that the shape, size and stability of AgNPs also depend on the pH value during the reaction [45]. The present results indicated that the different pH values of different species of *Ophiorrhiza* genus might also be provided some additional features to the generation of various size AgNPs using aqueous leaf extract of *Om*, *Oh* and *Or*.

3.2. X-ray diffraction analysis

Fig. 4 shows the XRD patterns of *Or*-AgNPs, *Om*-AgNPs and *Oh*-AgNPs synthesized nanoparticles by three *Ophiorrhiza* species extract. The diffraction peaks of the *Or*-AgNPs, *Om*-AgNPs and *Oh*-AgNPs were observed close to 28°, 32°, 38°, 44°, 46°, 55°, 57°, 64° and 77° in the 2θ range of 20°–80°, which can be ascribed to the (210), (122), (111), (200), (231), (142), (241), (220) and (311) silver crystalline planes of face-centered cubic structure (JCPDS, file No. 04–0783).

The crystallite size of AgNPs has been calculated using the Debye-Scherrer equation [46]:

$$D = \frac{k\lambda}{\beta \cos \theta}$$

where, D is the average crystallite size, k is the geometric factor (0.9), λ is the wavelength of X-ray radiation source (0.15406 nm) and β is the FWHM (full-width at half maximum) of the XRD peak at the diffraction angle θ and the results are presented in Table 1. The average crystallite size of *Om*-AgNPs, *Oh*-AgNPs and *Or*-AgNPs were 16 nm, 20 nm and 28 nm, respectively.

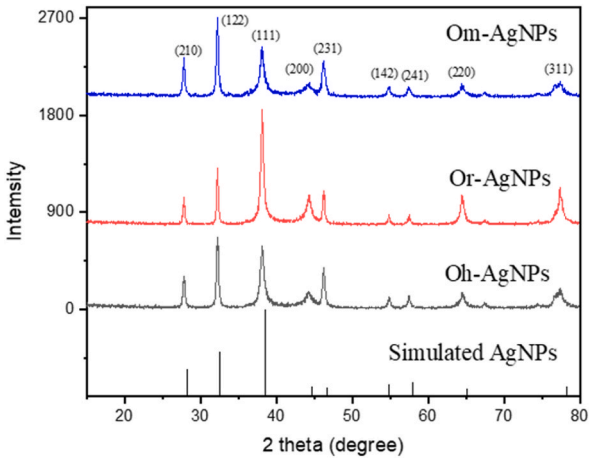

Fig. 4. XRD patterns of the synthesized AgNPs.

Table 1
X-ray powder diffraction results of synthesized AgNPs.

Sample	Plane (*hkl*)	2 Theta (°)	FWHM	Crystallite size, D (nm)	Average size (nm)
Om-AgNPs	[210]	27.8	0.34	25.4	16.3
	[122]	32.2	0.32	27.1	
	[111]	38.0	0.68	12.9	
	[200]	44.2	1.13 (7)	7.9	
	[231]	46.2	0.54	16.7	
	[142]	54.7	0.48	19.5	
	[241]	57.4	0.56	16.9	
	[220]	64.4	0.87	11.3	
	[311]	77.1	1.18	9.0	
Oh-AgNPs	[210]	27.79	0.33	25.8	20.0
	[122]	32.22	0.29	29.9	
	[111]	38.14	0.54	16.3	
	[200]	44.34	1.07	8.4	
	[231]	46.27	0.36	25.0	
	[142]	54.81	0.48	19.5	
	[241]	57.50	0.47	20.2	
	[220]	64.48	0.38	25.8	
	[311]	77.19	1.19	8.9	
Or-AgNPs	[210]	27.79	0.29	29.5	27.7
	[122]	32.19	0.25	34.5	
	[111]	38.08	0.41	21.2	
	[200]	44.39	0.90	9.9	
	[231]	46.22	0.25	36.3	
	[142]	54.78	0.27	34.3	
	[241]	57.43	0.41	23.1	
	[220]	64.44	0.31	32.1	
	[311]	77.38	0.37	28.8	

3.3. SEM, TEM, EDX and SAED analysis

The morphology and size of synthesized AgNPs were identified using SEM and TEM analysis. Spherical agglomerates with variable sizes were found during SEM analysis (Fig. 5a–c). TEM images of synthesized AgNPs are shown in Fig. 6 a. The images also show spherical shapes with variable sizes. The particle size distribution graph (Fig. 6 b) shows the average size of *Om*-AgNPs, *Oh*-AgNPs and *Or*-AgNPs to be approximately 17 ± 5 nm, 22 ± 9 nm and 26 ± 10 nm, respectively, which is in well agreement with the calculated size from XRD (16 nm, 20 nm and 28 nm) and SPR band (18 nm, 22 nm 26 nm) analysis. The SAED pattern (Fig. 6 c) showed that the diffraction rings might be indexed as (210), (122), (111), (200), (231), (142), (241), (220), and (311) reflections, which correspond to face-centered cubic polycrystalline silver from inner to outer with minimal variations in d-spacing.

Energy Dispersive X-ray spectra (EDX) of synthesized AgNPs are shown in Fig. 7 (a - c) and the percentage of elemental compositions is summarized in Table 2. All synthesized AgNPs showed an intense sharp signal at 3 keV indicating the formation of AgNPs as silver elements typically exhibits a characteristic optical absorption peak owing to surface plasmon resonance [47]. The percentage of the silver elemental composition of *Om*-AgNPs (88.74%) and *Oh*-AgNPs (91.96%) is much higher than that of *Or*-AgNPs (64.91%). EDX profile also showed other weak signals due to oxygen and carbon (Table 2), indicating the presence of oxygen and carbon-containing biomolecules on the surface of the AgNPs [48,49]. Our findings are in line with the other reports [50,51].

3.4. FTIR analysis

The FTIR spectra of leaf extracts and synthesized AgNPs are shown in Fig. 8a–c. The spectra in all samples exhibited bands at ca. 1720 cm^{-1} due to the stretching vibration of the carbonyl group (C=O) [52]. The peaks were observed at ca. 1620 cm^{-1}, 1535 cm^{-1}, 1380 cm^{-1} and 1065 cm^{-1} due to C=C aromatic rings, C=C alkene, germinal methyls and ether linkages, respectively, indicating that the surface of synthesized AgNPs may contain terpenoids or flavanones [53,54]. On the other hand, the EDX profile of synthesized AgNPs confirmed the presence of oxygen within AgNPs, suggesting that the oxygen-containing biomolecules such as alcohol, carboxylic acid and ester groups, are encapsulated on the surface of as-synthesized AgNPs, confirmed by FTIR also earlier in this report. These results further confirmed the presence of phytoconstituents like flavanones or polyphenols or alkaloids on the surface of synthesized AgNPs which assisted in the reduction of Ag^{+} along with the stabilization of the surface of the AgNPs.

3.5. Antibacterial activity

To investigate the antibacterial activity of the AgNPs, three different sizes of AgNPs, *Or*-AgNPs, *Om*-AgNPs and *Oh*-AgNPs, where organic biomolecules like *Om-*, *Oh-* and *Or*-capped around the AgNPs were tested for antibacterial activity against 2 g-positive (*Staphylococcus aureus* and *Bacillus cereus*) and 2 g-negative (*Escherichia coli* and *Vibrio cholerae*) bacteria by varying concentration of AgNPs (100 μg/mL, 200 μg/mL and 300 μg/mL). As shown in Table 3, no clear zone of inhibition was found against *Staphylococcus*

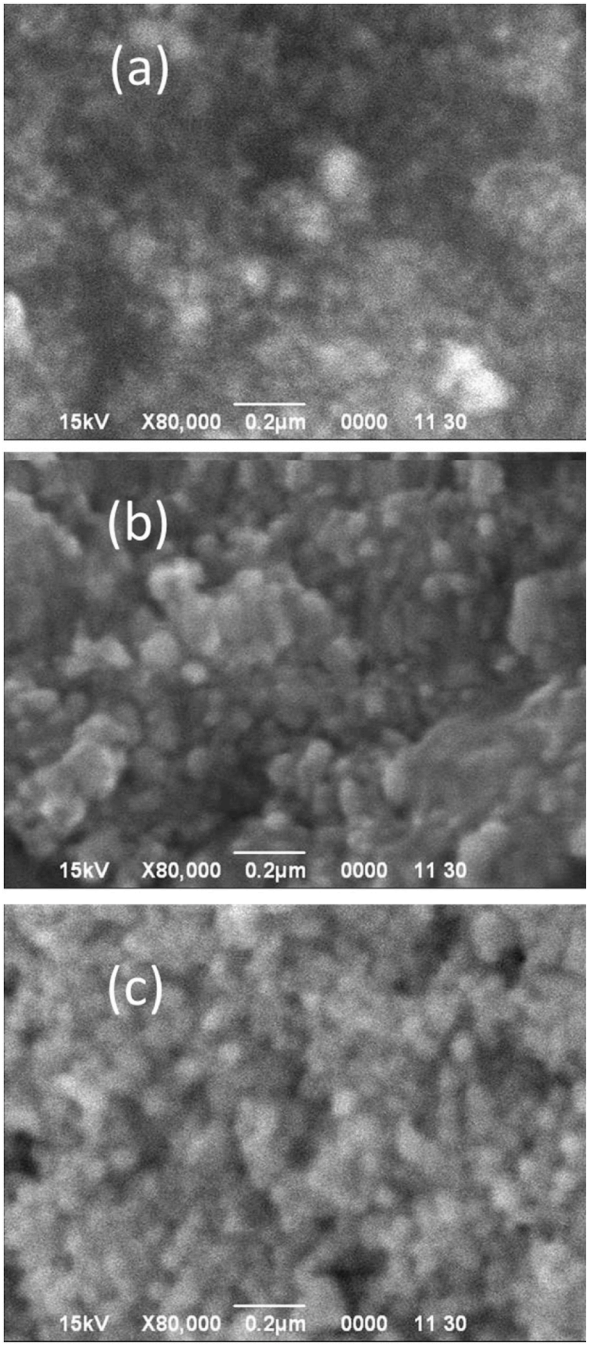

Fig. 5. Scanning electron micrographs of (a) *Om*-AgNPs, (b) *Oh*-AgNPs and (c) *Or*-AgNPs.

aureus while applying 100 µg/mL of AgNPs. With an increase in AgNPs concentration, the antibacterial activity increased. However, when compared in antibacterial activity of *Oh*-AgNPs and *Or*-AgNPs, the former afforded the broadest zone of inhibition against all four bacteria than the latter due to the highest content of silver in *Oh*-AgNPs (91.96% Ag) than *Or*-AgNPs (64.91% Ag). The antibacterial activity was also found to be influenced by the size of AgNPs, the larger size *Or*-AgNPs (26 nm) showed a lower zone of inhibition than lower size AgNPs, *Om*-AgNPs (18 nm) and *Oh*-AgNPs (22 nm) (Table 3), suggesting the concentration-dependent nature of AgNPs mediated bacterial death. A similar trend in concentration-dependent activity was observed by groups of researchers [55]. All three types of AgNPs showed the highest rate of inhibition against *Vibrio cholera* at a concentration of 100 µg/mL.

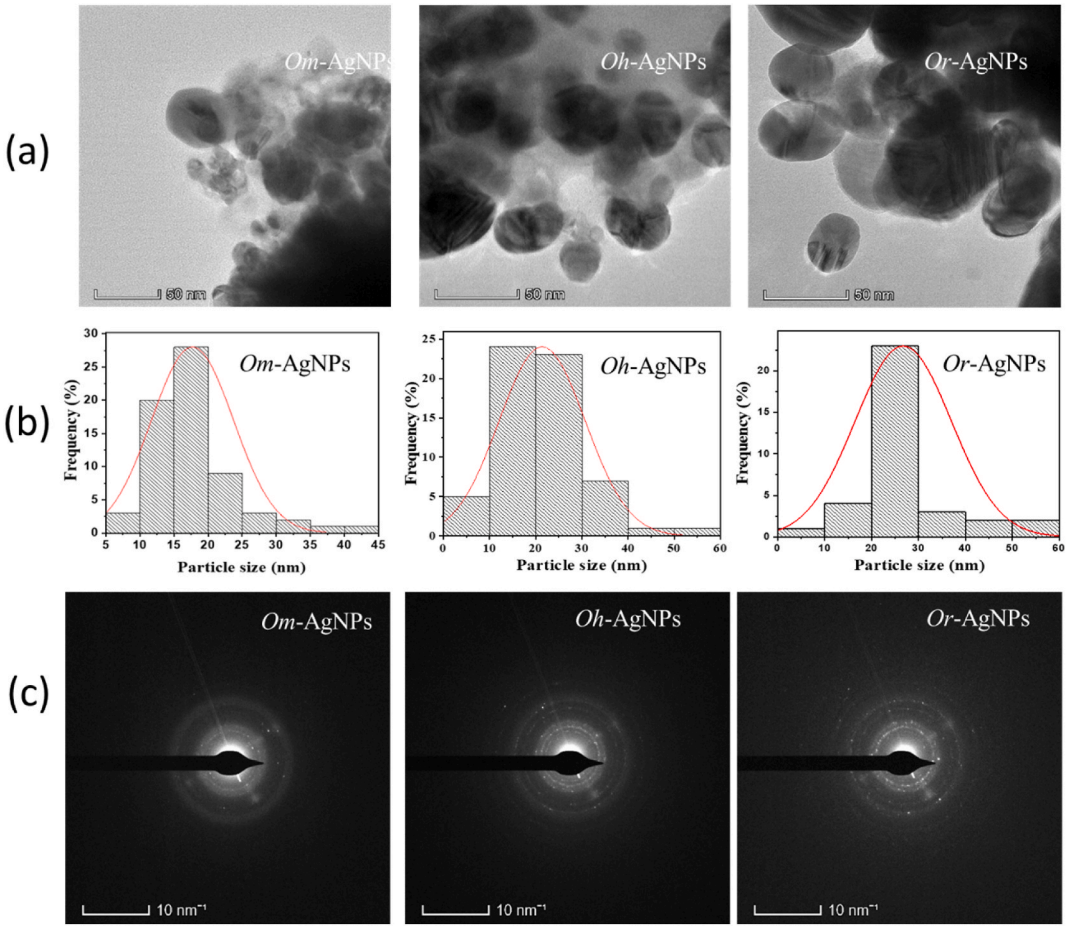

Fig. 6. (a) Transmission electron micrographs, (b) particle size distribution and (c) SAED pattern of *Om*-AgNPs, *Oh*-AgNPs and *Or*-AgNPs.

3.6. Antifungal activity

The antifungal activity of all three types of nano-size silver from 250 μg/mL to 400 μg/mL was examined against *Penicillium notatum* and *Aspergillus niger* using antifungal drug Nystatin as a positive control under similar control conditions. The synthesized AgNPs exhibited more activity than the standard antibiotic. The growth of *Penicillium notatum* was inhibited 60–80% with 250 μg/mL AgNPs concentration, whereas the inhibition (%) was observed to be less than 50% for *Aspergillus niger*. As the concentration of AgNPs increased, the inhibitory activities steadily increased (Fig. 9). However, the *Oh-AgNPs* exhibited higher antifungal activity against *Penicillium notatum* with 250 μg/mL AgNPs concentration than the other two synthesized AgNPs. Among them, *Om*-AgNPs showed minimum activity against these two fungi even though the size of the *Om*-AgNPs were less among the three AgNPs which is somewhat opposite to other reports [56,57]. This is probably due to the fact that biomolecules present on the surface of *Om*-AgNPs might be responsible for their minimum antifungal action. However, the results suggest that, AgNPs have the potential to be employed as antifungal agents possibly due to their ability to impair membrane integrity and cause cellular and organelle structural degradation, all of which are necessary for fungal growth and survival [58]. Similar studies have also been reported on fungal species, probably due to the solution's ability to saturate and adhere to the fungal hyphae with great intensity [59]. In addition, according to previous research, AgNPs are likely to cause damage to the transport system, resulting in the efflux of intracellular ions and the accumulation of silver ions, as well as the inhibition of metabolic and respiratory activities [60,61]. Although the mechanism is not clear in our study, the present results imply that AgNPs have significant antifungal efficacy, deserving further study for clinical applications.

4. Conclusions

In the work, using leaf extracts of *Ophiorrhiza mungos*, *Ophiorrhiza harrisiana* and *Ophiorrhiza rugosa*, we described a simple, efficient and eco-friendly greener route to synthesize different particle sizes of AgNPs. The biosynthesized AgNPs were spherical in shape and highly stable. The mean sizes of AgNPs were 17 ± 5 nm, 22 ± 9 nm and 26 ± 10 nm for *Om*-AgNPs, *Oh*-AgNPs and *Or*-AgNPs, respectively. Size-dependent antibacterial activity was observed. Though high antibacterial activity was found in all three types of

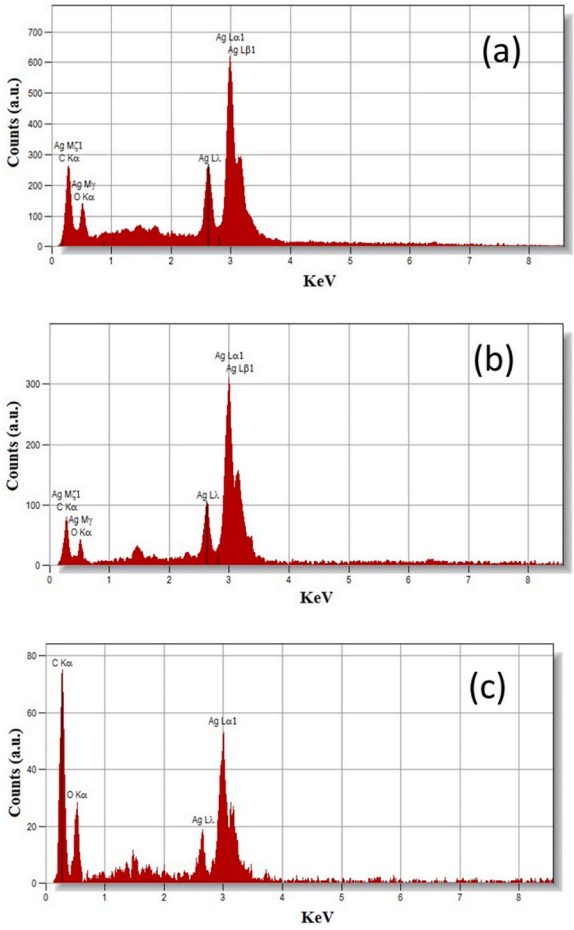

Fig. 7. EDX spectra of (a) *Om*-AgNPs, (b) *Oh*-AgNPs and (c) *Or*-AgNPs.

Table 2
Chemical analysis of synthesized AgNPs using EDX analysis.

Sample	Weight (%)		
	Ag	O	C
Om-AgNPs	64.91	22.46	12.63
Oh-AgNPs	88.74	7.64	3.62
Or-AgNPs	91.96	5.71	2.33

AgNPs, the highest antibacterial activity was observed in the case of *Vibrio cholera.* In addition, antifungal activity was evident with notable inhibition for all three types of AgNPs where *Oh*-AgNPs were most lethal to the fungus used in this study. This study describes the nano-size-control synthesis of AgNPs using aqueous plant extracts for the first time from the same genus of *Ophiorrhiza* species. These synthesized AgNPs demonstrated potential biological applications and warrant further study of the role of biomolecules in the synthesis of nano-sized AgNPs and their antimicrobial potential via multifaceted mechanisms and binding sites. Furthermore, size-dependent activities like catalytic, optical, electrical and sensing activity can also be the potential subject to be explored. It can also be concluded that the present study might be taken as a baseline study for the size-controlled synthesis by varying species within the same genus. We believe this plant extract based synthesis of metal nanoparticles of a controlled size will be promising synthesis route for various fields, including biomedicine.

Author contribution statement

Sumon Ganguli: Conceived and designed the experiments; Performed the experiments; Analyzed and interpreted the data; Wrote the paper.

Sabbir Howlader: Conceived and designed the experiments; Performed the experiments.

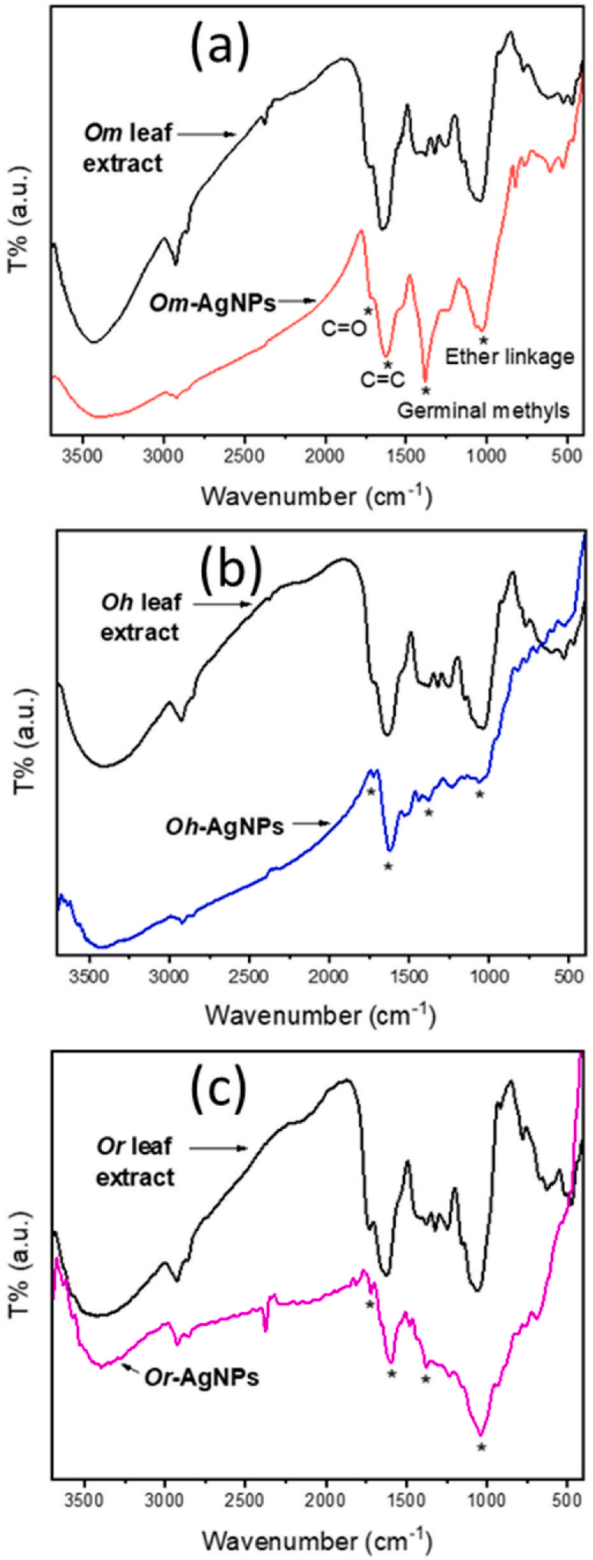

Fig. 8. FTIR spectra of leaf extracts of *Ophiorrhiza* genus species and synthesized AgNPs: (a) *Om*-AgNPs, (b) *Oh*-AgNPs and (c) *Or*-AgNPs.

Table 3
Zone of Inhibition (mm) for *Or*-AgNPs, *Om*-AgNPs and *Oh*-AgNPs tested against different gram-positive and gram-negative bacteria.

Microorganisms	Antibacterial agent	Zone of inhibition (mm) [for different concentrations of AgNPs Suspension]			Negative Control[a]	Positive Control[a]
		100 μg/mL	200 μg/mL	300 μg/mL		
Staphylococcus aureus	*Or*-AgNPs	0	7	7	0	31
	Om-AgNPs	0	7	7		
	Oh-AgNPs	0	8	9		
Bacillus cereus	*Or*-AgNPs	0	6	7	0	26
	Om-AgNPs	0	6	6		
	Oh-AgNPs	7	7	7		
Escherichia coli	*Or*-AgNPs	0	6	7	0	26
	Om-AgNPs	0	6	6		
	Oh-AgNPs	7	7	7		
Vibrio cholerae	*Or*-AgNPs	7	7	10	0	32
	Om-AgNPs	9	9	11		
	Oh-AgNPs	8	8	11		

[a] Chloramphenicol and deionized water were used as positive and negative control, respectively.

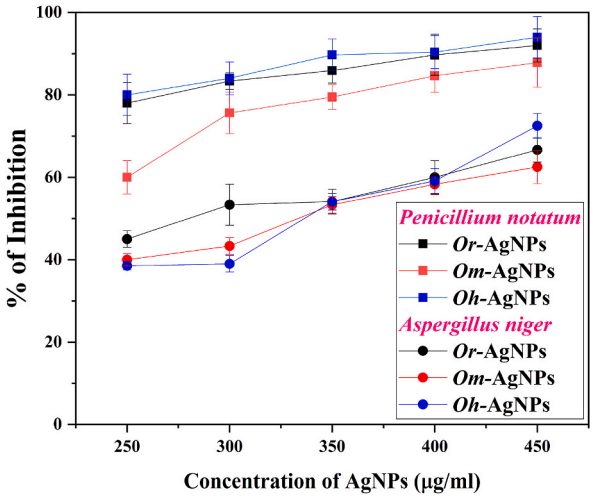

Fig. 9. Antifungal activity of the synthesized AgNPs.

A.K.M. Atique Ullah, Farhana Rumzum Bhuiyan: Contributed reagents, materials, analysis tools or data.

Aklima A Akhia, Abid Hasan, Kamol Dey: Analyzed and interpreted the data; Contributed reagents, materials, analysis tools or data.

Saiful Islam, Ferdousi Ali, Ashok Kumar Chakraborty: Performed the experiments; Analyzed and interpreted the data.

Samiran Bhattacharjee, Benu Kumar Dey: Conceived and designed the experiments; Analyzed and interpreted the data; Contributed reagents, materials, analysis tools or data; Wrote the paper.

Data availability statement

Data included in article/supp. Material/referenced in article.

Declaration of competing interest

The authors declare that they have no known competing financial interests or personal relationships that could have appeared to influence the work reported in this paper

Acknowledgments

The authors gratefully acknowledge the financial support by the BUGC postdoctoral fellowship program from the Bangladesh University Grants Commission (BUGC). We also acknowledge the support from Centre for Advanced Research in Sciences (University of Dhaka), Research and Publication Cell (University of Chittagong) and Ministry of Education (Bangladesh). In addition, the authors acknowledge Bithi Mojumder, Assistant Professor Department of English, Noakhali Science and Technology University, Bangladesh for

her assistance in English language editing.

References

[1] J. Huang, Y. Tao, S. Ran, Y. Yang, C. Li, P. Luo, Z. Chen, X. Tan, A hydroxy-containing three dimensional covalent organic framework bearing silver nanoparticles for reduction of 4-nitrophenol and degradation of organic dyes, New J. Chem. 46 (2022) 17153–17160, https://doi.org/10.1039/D2NJ02437C.

[2] R. Ettlinger, U. Lachelt, R. Gref, P. Horcajada, T. Lammers, C. Serre, P. Couvreur, R.E. Morris, S. Wuttke, Toxicity of metal–organic framework nanoparticles: from essential analyses to potential applications, Chem. Soc. Rev. 51 (2022) 464–484, https://doi.org/10.1039/D1CS00918D.

[3] I. Khan, K. Saeed, I. Khan, Nanoparticles: properties, applications and toxicities, arab, J. Chem. 12 (2019) 908–931, https://doi.org/10.1016/J.ARABJC.2017.05.011.

[4] N. Baig, I. Kammakakam, W. Falath, I. Kammakakam, Nanomaterials: a review of synthesis methods, properties, recent progress, and challenges, Mater, Advisor 2 (2021) 1821–1871, https://doi.org/10.1039/D0MA00807A.

[5] S.M. Mousavi, S.A. Hashemi, Y. Ghasemi, A. Atapour, A.M. Amani, A. Savar Dashtaki, A. Babapoor, O. Arjmand, Green synthesis of silver nanoparticles toward bio and medical applications: review study, Artif. Cells, Nanomed. Biotechnol. 46 (2018), https://doi.org/10.1080/21691401.2018.1517769. S855–S872.

[6] N. Hossain, M.A. Islam, M.A. Chowdhury, Synthesis and characterization of plant extracted silver nanoparticles and advances in dental implant applications, Heliyon 8 (2022), e12313, https://doi.org/10.1016/J.HELIYON.2022.E12313.

[7] T. Bruna, F. Maldonado-Bravo, P. Jara, N. Caro, Silver nanoparticles and their antibacterial applications, Int. J. Mol. Sci. 22 (2021), https://doi.org/10.3390/IJMS22137202.

[8] J.T. Seil, T.J. Webster, Antimicrobial applications of nanotechnology: methods and literature, Int. J. Nanomed. 7 (2012) 2767–2781, https://doi.org/10.2147/IJN.S24805.

[9] A. Ivask, A. Elbadawy, C. Kaweeteerawat, D. Boren, H. Fischer, Z. Ji, C.H. Chang, R. Liu, T. Tolaymat, D. Telesca, J.I. Zink, Y. Cohen, P.A. Holden, H.A. Godwin, Toxicity mechanisms in Escherichia coli vary for silver nanoparticles and differ from ionic silver, ACS Nano 8 (2014) 374–386, https://doi.org/10.1021/NN4044047.

[10] K. Moorthy, K.C. Chang, P.J. Yu, W.J. Wu, M.Y. Liao, H.C. Huang, H.C. Chien, C.K. Chiang, Synergistic actions of phytonutrient capped nanosilver as a novel broad-spectrum antimicrobial agent: unveiling the antibacterial effectiveness and bactericidal mechanism, New J. Chem. 46 (2022) 15301–15312, https://doi.org/10.1039/D2NJ02469A.

[11] S. Sankar Sana, R. Haldhar, J. Parameswaranpillai, M. Chavali, S.C. Kim, Silver nanoparticles-based composite for dye removal: a comprehensive review, Clean. Mater. 6 (2022), 100161, https://doi.org/10.1016/J.CLEMA.2022.100161.

[12] Y. Park, New paradigm shift for the green synthesis of antibacterial silver nanoparticles utilizing plant extracts, Toxicol. Res. 30 (2014) 169, https://doi.org/10.5487/TR.2014.30.3.169.

[13] S.N. Nandhini, N. Sisubalan, A. Vijayan, C. Karthikeyan, M. Gnanaraj, D.A.M. Gideon, T. Jebastin, K. Varaprasad, R. Sadiku, Recent advances in green synthesized nanoparticles for bactericidal and wound healing applications, Heliyon 9 (2023), https://doi.org/10.1016/J.HELIYON.2023.E13128.

[14] A.S. Eltaweil, A.M. Abdelfatah, M. Hosny, M. Fawzy, Novel biogenic synthesis of a Ag@Biochar nanocomposite as an antimicrobial agent and photocatalyst for methylene blue degradation, ACS Omega 7 (2022) 8046–8059, https://doi.org/10.1021/ACSOMEGA.1C07209.

[15] D. Hu, X. Yang, W. Chen, Z. Feng, C. Hu, F. Yan, X. Chen, D. Qu, Z. Chen, Rhodiola rosea Rhizome extract-mediated green synthesis of silver nanoparticles and evaluation of their potential antioxidant and catalytic reduction activities, ACS Omega 6 (2021) 24450–24461, https://doi.org/10.1021/ACSOMEGA.1C02843.

[16] F. Ahmed, I. Ali, H.S. Ali, S. Yasmeen, S. Ullah, S. Burki, M. Adil, J. Nisar, M.R. Shah, Synthesis and characterization of a plant growth regulator based silver nanoparticles for the ultrasensitive detection of environmentally toxic Hg2+ ions in tap water, New J. Chem. 45 (2021) 18039–18047, https://doi.org/10.1039/D1NJ03393J.

[17] E.O. Mikhailova, Silver nanoparticles: mechanism of action and probable bio-Application, J. Funct. Biomater. 11 (2020), https://doi.org/10.3390/JFB11040084.

[18] X. Wei, F. Cheng, Y. Yao, X. Yi, B. Wei, H. Li, Y. Wu, J. He, Facile synthesis of a carbon dots and silver nanoparticles (CDs/AgNPs) composite for antibacterial application, RSC Adv. 11 (2021) 18417–18422, https://doi.org/10.1039/D1RA02600C.

[19] N.K. Sharma, J. Vishwakarma, S. Rai, T.S. Alomar, N. Almasoud, A. Bhattarai, Green route synthesis and characterization techniques of silver nanoparticles and their biological adeptness, ACS Omega 7 (2022) 27004–27020, https://doi.org/10.1021/ACSOMEGA.2C01400.

[20] C. Vanlalveni, S. Lallianrawna, A. Biswas, M. Selvaraj, B. Changmai, S.L. Rokhum, Green synthesis of silver nanoparticles using plant extracts and their antimicrobial activities: a review of recent literature, RSC Adv. 11 (2021) 2804–2837, https://doi.org/10.1039/D0RA09941D.

[21] M.S. Nawabjohn, P. Sivaprakasam, S.K. Anandasadagopan, A.A. Begum, A.K. Pandurangan, Green synthesis and characterisation of silver nanoparticles using Cassia tora seed extract and investigation of antibacterial potential, Appl. Biochem. Biotechnol. 194 (2022) 464–478, https://doi.org/10.1007/S12010-021-03651-4/FIGURES/8.

[22] D. Chugh, V.S. Viswamalya, B. Das, Green synthesis of silver nanoparticles with algae and the importance of capping agents in the process, J. Genet. Eng. Biotechnol. 191 (19) (2021) 1–21, https://doi.org/10.1186/S43141-021-00228-W.

[23] N.S. Alharbi, N.S. Alsubhi, A.I. Felimban, Green synthesis of silver nanoparticles using medicinal plants: characterization and application, J. Radiat. Res. Appl. Sci. 15 (2022) 109–124, https://doi.org/10.1016/J.JRRAS.2022.06.012.

[24] S. Ahmad, S. Munir, N. Zeb, A. Ullah, B. Khan, J. Ali, M. Bilal, M. Omer, M. Alamzeb, S.M. Salman, S. Ali, Green nanotechnology: a review on green synthesis of silver nanoparticles — an ecofriendly approach, Int. J. Nanomed. 14 (2019) 5087–5107, https://doi.org/10.2147/IJN.S200254.

[25] S. Hamedi, S.A. Shojaosadati, Rapid and green synthesis of silver nanoparticles using Diospyros lotus extract: evaluation of their biological and catalytic activities, Polyhedron 171 (2019) 172–180, https://doi.org/10.1016/J.POLY.2019.07.010.

[26] M. Taher, S.S. Shaari, D. Susanti, D. Arbain, Z.A. Zakaria, Genus Ophiorrhiza: a Review of its distribution, traditional uses, phytochemistry, biological activities and propagation, Mol 25 (2020) 2611, https://doi.org/10.3390/MOLECULES25112611.

[27] W. Pajerski, P. Chytrosz-Wrobel, M. Golda-Cepa, M. Pawlyta, W. Reczynski, D. Ochonska, M. Brzychczy-Wloch, A. Kotarba, Opposite effects of gold and silver nanoparticle decoration of graphenic surfaces on bacterial attachment, New J. Chem. 46 (2022) 13286–13295, https://doi.org/10.1039/D2NJ00648K.

[28] J. Ma, K. Li, S. Gu, Y. Wu, J. Zhang, J. Wu, L. Zhao, X. Li, Antimicrobial carbon-dot–stabilized silver nanoparticles, New J. Chem. 46 (2022) 2546–2552, https://doi.org/10.1039/D1NJ05798G.

[29] Y. Dong, H. Zhu, Y. Shen, W. Zhang, L. Zhang, Antibacterial activity of silver nanoparticles of different particle size against Vibrio Natriegens, PLoS One 14 (2019), https://doi.org/10.1371/JOURNAL.PONE.0222322.

[30] E.A. Skomorokhova, T.P. Sankova, I.A. Orlov, A.N. Savelev, D.N. Magazenkova, M.G. Pliss, A.N. Skvortsov, I.M. Sosnin, D.A. Kirilenko, I.V. Grishchuk, E. I. Sakhenberg, E.V. Polishchuk, P.N. Brunkov, A.E. Romanov, L.V. Puchkova, E.Y. Ilyechova, Size-Dependent bioactivity of silver nanoparticles: antibacterial properties, influence on copper status in mice, and whole-body turnover, Nanotechnol. Sci. Appl. 13 (2020) 137–157, https://doi.org/10.2147/NSA.S287658.

[31] R.M.C.R. Ramos, M.D. Regulacio, Controllable synthesis of bimetallic nanostructures using biogenic reagents: a green perspective, ACS Omega 6 (2021) 7212–7228, https://doi.org/10.1021/ACSOMEGA.1C00692.

[32] Y.W. Hartati, S.N. Topkaya, S. Gaffar, H.H. Bahti, A.E. Cetin, Synthesis and characterization of nanoceria for electrochemical sensing applications, RSC Adv. 11 (2021) 16216–16235, https://doi.org/10.1039/D1RA00637A.

[33] R. Javed, M. Zia, S. Naz, S.O. Aisida, N. ul Ain, Q. Ao, Role of capping agents in the application of nanoparticles in biomedicine and environmental remediation: recent trends and future prospects, J. Nanobiotechnol. 18 (2020) 1–15, https://doi.org/10.1186/S12951-020-00704-4.

[34] A. Nene, M. Galluzzi, L. Hongrong, P. Somani, S. Ramakrishna, X.F. Yu, Synthetic preparations and atomic scale engineering of silver nanoparticles for biomedical applications, Nanoscale 13 (2021) 13923–13942, https://doi.org/10.1039/D1NR01851E.

[35] M. Adnan, M.N.U. Chy, A.T.M.M. Kamal, M. Azad, A. Paul, S. Uddin, J. Barlow, M. Faruque, C. Park, D. Cho, Investigation of the biological activities and characterization of bioactive constituents of Ophiorrhiza rugosa var. prostrata (D.Don) & amp; Mondal Leaves through in Vivo, in Vitro, and in Silico Approaches, Molecules 24 (2019) 1367.
[36] C.D. Yang, X.Z. He, G.Q. Gou, Ophiorrhiza guizhouensis (Rubiaceae), a new species from Guizhou Province, southwestern China, PhytoKeys (2018) 121, https://doi.org/10.3897/PHYTOKEYS.95.22506.
[37] G. Krishnakumar, K.P. Dintu, S.C. Varghese, D.S. Nair, G. Gopinath, K.B. Rameshkumar, K. Satheeshkumar, P.N. Krishnan, Ophiorrhiza, A promising herbaceous source of the anticancer compound camptothecin, Plant Sci. Today. 7 (2020) 240–250, https://doi.org/10.14719/PST.2020.7.2.660.
[38] G. Gopinath, B. Jose, P. Ravichandran, K. Satheeshkumar, Tissue culture of Ophiorrhiza mungos L., a prospective method for the production of an anticancer drug, camptothecin, Plant Sci. Today. 5 (2018) 1–8, https://doi.org/10.14719/PST.2018.5.1.359.
[39] M. Malik, M.A. Iqbal, M. Malik, M.A. Raza, W. Shahid, J.R. Choi, P.V. Pham, Biosynthesis and characterizations of silver nanoparticles from Annona squamosa leaf and fruit extracts for size-dependent biomedical applications, Nanomaterials 12 (2022), https://doi.org/10.3390/NANO12040616.
[40] A.K.M.A. Ullah, M.F. Kabir, M. Akter, A.N. Tamanna, A. Hossain, A.R.M. Tareq, M.N.I. Khan, A.K.M.F. Kibria, M. Kurasaki, M.M. Rahman, Green synthesis of bio-molecule encapsulated magnetic silver nanoparticles and their antibacterial activity, RSC Adv. 8 (2018) 37176–37183, https://doi.org/10.1039/C8RA06908E.
[41] I.J.B. Durval, H.M. Meira, B.O. de Veras, R.D. Rufino, A. Converti, L.A. Sarubbo, Green synthesis of silver nanoparticles using a biosurfactant from Bacillus cereus UCP 1615 as stabilizing agent and its application as an antifungal Agent, Fermentatio 7 (2021) 233, https://doi.org/10.3390/FERMENTATION7040233.
[42] S. Priya, A. Murali, D.R. Preeth, K.C. Dharanibalaji, G. Jeyajothi, Green synthesis of silver nanoparticle-embedded poly(methyl methacrylate-co-methacrylic acid) copolymer for fungal-free leathers, Polym. Bull. 79 (2022) 4607–4626, https://doi.org/10.1007/S00289-021-03714-W/FIGURES/12.
[43] D. Cruz, P.L. Falé, A. Mourato, P.D. Vaz, M. Luisa Serralheiro, A.R.L. Lino, Preparation and physicochemical characterization of Ag nanoparticles biosynthesized by Lippia citriodora (Lemon Verbena), Colloids Surf., B 81 (2010) 67–73, https://doi.org/10.1016/J.COLSURFB.2010.06.025.
[44] E. Saion, E. Gharibshahi, K. Naghavi, Size-controlled and optical properties of monodispersed silver nanoparticles synthesized by the radiolytic reduction method, Int. J. Mol. Sci. 14 (2013) 7880, https://doi.org/10.3390/IJMS14047880.
[45] S.S. Birla, S.C. Gaikwad, A.K. Gade, M.K. Rai, Rapid synthesis of silver nanoparticles from Fusarium oxysporum by optimizing physicocultural conditions, Sci. World J. 2013 (2013), https://doi.org/10.1155/2013/796018.
[46] B. Kumar, K.S. Vizuete, V. Sharma, A. Debut, L. Cumbal, Ecofriendly synthesis of monodispersed silver nanoparticles using Andean Mortiño berry as reductant and its photocatalytic activity, Vacuum 160 (2019) 272–278, https://doi.org/10.1016/J.VACUUM.2018.11.027.
[47] G.A. Alamu, O. Adedokun, I.T. Bello, Y.K. Sanusi, Plasmonic enhancement of visible light absorption in Ag-TiO2 based dye-sensitized solar cells, Chem. Phys. Impact. 3 (2021), 100037, https://doi.org/10.1016/J.CHPHI.2021.100037.
[48] M.F. Baran, C. Keskin, A. Baran, A. Hatipoglu, M. Yildiztekin, S. Kucukaydin, K. Kurt, H. Hosgoren, M.M.R. Sarker, A. Sufianov, O. Beylerli, R. Khalilov, A. Eftekhari, Green synthesis of silver nanoparticles from Allium cepa L. Peel extract, their antioxidant, antipathogenic, and anticholinesterase activity, Molecules 28 (2023) 2310, https://doi.org/10.3390/MOLECULES28052310.
[49] A.K. Sidhu, N. Verma, P. Kaushal, Role of biogenic aapping agents in the synthesis of metallic nanoparticles and evaluation of their therapeutic potential, Front. Nanotechnol. 3 (2022) 105, https://doi.org/10.3389/FNANO.2021.801620/BIBTEX.
[50] A.G. Femi-Adepoju, A.O. Dada, K.O. Otun, A.O. Adepoju, O.P. Fatoba, Green synthesis of silver nanoparticles using terrestrial fern (Gleichenia Pectinata (Willd.) C. Presl.): characterization and antimicrobial studies, Heliyon 5 (2019) 1543, https://doi.org/10.1016/J.HELIYON.2019.E01543.
[51] K.M.F. Hasan, L. Xiaoyi, Z. Shaoqin, P.G. Horvath, M. Bak, L. Bejo, G. Sipos, T. Alpar, Functional silver nanoparticles synthesis from sustainable point of view: 2000 to 2023 – A review on game changing materials, Heliyon 8 (2022), e12322, https://doi.org/10.1016/J.HELIYON.2022.E12322.
[52] S. Taheri, M.M. Heravi, P. Mohammadi, Synthesis of Ag nanoparticles by Celery leaves extract supported on magnetic biochar substrate, as a catalyst for the reduction reactions, Sci. Rep. 12 (2022) 1–11, https://doi.org/10.1038/s41598-022-18131-w.
[53] K. Logaranjan, A.J. Raiza, S.C.B. Gopinath, Y. Chen, K. Pandian, Shape- and size-controlled synthesis of silver nanoparticles using Aloe vera plant extract and their antimicrobial activity, Nanoscale Res. Lett. 11 (2016), https://doi.org/10.1186/S11671-016-1725-X.
[54] A.O. Dada, F.A. Adekola, F.E. Dada, A.T. Adelani-Akande, M.O. Bello, C.R. Okonkwo, A.A. Inyinbor, A.P. Oluyori, A. Olayanju, K.O. Ajanaku, C.O. Adetunji, Silver nanoparticle synthesis by Acalypha wilkesiana extract: phytochemical screening, characterization, influence of operational parameters, and preliminary antibacterial testing, Heliyon 5 (2019), e02517, https://doi.org/10.1016/J.HELIYON.2019.E02517.
[55] M. Asimuddin, M.R. Shaik, S.F. Adil, M.R.H. Siddiqui, A. Alwarthan, K. Jamil, M. Khan, Azadirachta indica based biosynthesis of silver nanoparticles and evaluation of their antibacterial and cytotoxic effects, J. King Saud Univ. Sci. 32 (2020) 648–656, https://doi.org/10.1016/J.JKSUS.2018.09.014.
[56] N. Duran, M. Duran, M.B. de Jesus, A.B. Seabra, W.J. Favaro, G. Nakazato, Silver nanoparticles: a new view on mechanistic aspects on antimicrobial activity, Nanomed. Nanotechnol. Biol. Med. 12 (2016) 789–799, https://doi.org/10.1016/J.NANO.2015.11.016.
[57] E. Matras, A. Gorczyca, S.W. Przemieniecki, M. Ocwieja, Surface properties-dependent antifungal activity of silver nanoparticles, Sci. Rep. 121 (12) (2022) 1–17, https://doi.org/10.1038/s41598-022-22659-2.
[58] L. Li, H. Pan, L. Deng, G. Qian, Z. Wang, W. Li, C. Zhong, The antifungal activity and mechanism of silver nanoparticles against four pathogens causing kiwifruit post-harvest rot, Front. Microbiol. 13 (2022), https://doi.org/10.3389/FMICB.2022.988633/FULL.
[59] K.J. Kim, W.S. Sung, B.K. Suh, S.K. Moon, J.S. Choi, J.G. Kim, D.G. Lee, Antifungal activity and mode of action of silver nano-particles on Candida albicans, Biometals 22 (2009) 235–242, https://doi.org/10.1007/S10534-008-9159-2.
[60] J.R. Morones, J.L. Elechiguerra, A. Camacho, K. Holt, J.B. Kouri, J.T. Ramirez, M.J. Yacaman, The bactericidal effect of silver nanoparticles, Nanotechnology 16 (2005) 2346–2353, https://doi.org/10.1088/0957-4484/16/10/059.
[61] H. Du, T.M. Lo, J. Sitompul, M.W. Chang, Systems-level analysis of Escherichia coli response to silver nanoparticles: the roles of anaerobic respiration in microbial resistance, Biochem. Biophys. Res. Commun. 424 (2012) 657–662, https://doi.org/10.1016/J.BBRC.2012.06.134.